

1 **TD-MP: A Max Pressure Algorithm Considering Delay Equity**
2

3 **Hao Liu***
4 Postdoctoral Scholar
5 Department of Civil and Environmental Engineering
6 The Pennsylvania State University
7 College Park, PA, 168082
8 Email: hfl5376@psu.edu
9

10 **Vikash V. Gayah**
11 Associate Professor
12 Department of Civil and Environmental Engineering
13 The Pennsylvania State University
14 College Park, PA, 168082
15 Email: gayah@engr.psu.edu
16

17 * Corresponding author
18

19 Word Count: 7395 words
20

21 Submitted July 2022
22
23

1 **ABSTRACT**

2 This paper proposes a novel decentralized signal control algorithm that seeks to improve traffic delay
3 equity, measured as the variation of delay experienced by individual vehicles. The proposed method extends
4 the recently developed delay-based Max Pressure (D-MP) algorithm by using the sum of cumulative delay
5 experienced by all vehicles that joined a given link as the metric for weight calculation. Doing so ensures
6 the movements with lower traffic loads have a higher chance of being served as their delay increases. Three
7 existing MP models are used as baseline models with which to compare the proposed algorithm in
8 microscopic simulations of both a single intersection and a grid network. The results indicate that the
9 proposed algorithm can improve the delay equity for various traffic conditions, especially for the highly
10 unbalanced traffic flows. Moreover, this improvement in delay equity does not come with a significant
11 increase to average delay experienced by all vehicles. In fact, the average delay from the proposed algorithm
12 is close to – and sometimes even lower than – the baseline models. Therefore, the proposed algorithm can
13 maintain both objectives at the same time. In addition, the performance of the proposed control strategy
14 was tested in a connected vehicle environment. The results show that the proposed algorithm outperforms
15 the other baseline models in both reducing traffic delay and increasing delay equity when the penetration
16 rate is less or equal to 60%, which would not be exceeded in reality in the near future.

17

18 **Keywords:** Adaptive Signal Control, Max Pressure, Decentralized, Delay Equity, Connected Vehicles

1 **INTRODUCTION AND BACKGROUND**

2 Traffic signals serve as one of the most used tools to manage conflicting vehicle movements at intersections.
 3 However, they also serve as the main bottleneck that impedes the network mobility since they directly stop
 4 vehicles and impose travel delays (1). Hence, proposing design of signal timing is required to ensure
 5 efficient traffic operations at signalized intersections. Adaptive signal control methods use real-time traffic
 6 measurements to predict how traffic patterns will evolve and then optimize the signal timing based on
 7 prevailing patterns and/or these predictions. It has been studied vastly in the past decades and regarded as
 8 a promising technique to improve the network mobility (2–5). However, it remains a challenging research
 9 topic, especially for the network-wide signal control problems due to its complexity. One difficulty is to
 10 accurately model the temporospatial interdependence between intersection performance. Another is the
 11 computational speed to solve a complex optimization problem in real time. Decentralized traffic signal
 12 control algorithms address both concerns since it optimizes signal timings for each intersection based only
 13 on local traffic conditions. Many decentralized traffic signal control approaches have been proposed in the
 14 past decades, such as OPAC (6), RHODES (2), SCOOT (7), etc. A comparison between centralized and
 15 decentralized control approaches can be found in (8).

16 The max-pressure (MP) signal control algorithm, also known as backpressure (BP), is a
 17 decentralized optimization algorithm that was originally proposed for the routing and scheduling of packet
 18 transmission in a wireless network (9). Varaiya (10) was the first to implement MP in traffic signal control
 19 problems, which we refer to as the Original-MP in the rest of this paper. The MP algorithm requires turning
 20 ratio and saturation flows at an intersection be known, but does not require any knowledge of demand
 21 information. Due to its implementation ease and decentralized nature, numerous studies have proposed
 22 and/or tested the performance of variants of MP in signalized street networks; see (11–25) for examples.
 23 The basic steps of a MP algorithm are as follows:

- 24 1. A selected metric is measured for each vehicle movement at an intersection at each instance
 25 when signal needs to be updated. Metrics that are commonly used include queue length, travel
 26 time and traffic delay.
- 27 2. The weight of each movement is computed as this measured metric minus the average value of
 28 this metrics for all downstream movements.
- 29 3. The pressure of a signal phase is computed as the sum of the weights multiplied by the
 30 saturation flows of the movements served during that phase.
- 31 4. The pressure is then used to change the signal phasing and timing plan. For cycleless
 32 implementation, the phase with the maximum pressure is activated for the next time step. When
 33 a specific cycle length is to be maintained, the phase splits for the next cycle are determined
 34 based on the proportion of the pressures.

35 The control performance highly depends on the selection of the metric. The Original-MP uses
 36 ‘queue length’ as the metric for weight calculation. However, it also uses point queue models to represent
 37 the traffic state on links and store-and-forward models to depict the vehicle transitions between links. Since
 38 the vehicles join the point queue immediately once they enter the link, this model does not track the
 39 positions and moving status of vehicles. Therefore, it should be emphasized that the ‘queue length’ in the
 40 Original-MP represents the number of vehicles on the link as as opposed to the number of vehicles stopped
 41 in a queue. In addition, it assumes the queue storage capacity is infinite, which is problematic when the
 42 traffic volume is high. To address these issues, many queue-based MP variants have been proposed. Xiao
 43 et al. (14) proposed a *pressure releasing policy* (PRP) that considers both the local queue length and the
 44 queues on the entry links. The latter was used to adjust the weight while accounting for queue capacity.
 45 Another method is normalizing queue lengths using queue capacities (18, 25). Gregoire et al. (12) used a
 46 convex function of queue capacity to normalize the queue length, which outperforms the Original-MP under
 47 heavy traffic conditions. Although these methods normalize or adjust the number of vehicles for the weight
 48 calculation to reduce queue spillovers, one drawback is that vehicles’ positions and moving status are not
 49 considered. For example, a vehicle stopped in a queue close to the stop line should weigh more than a free

flow moving vehicle far away from the intersection. To address this, Li and Jabari (21) proposed a *position weighted backpressure* (PWBP) algorithm which uses the sum of normalized distance over all vehicles on a link to define the weight of a movement. For an upstream movement, the normalized distance is the actual distance from the upstream end of the link divided by the link length, which means a vehicle closer to the intersection has higher weight. For the downstream movement, the actual distance from the downstream end of the link is normalized. This method generates low weight if the downstream vehicles are closer to the intersection and thus can reduce the occurrence of queue spillover. Most of the MP variants switch phases at a pre-defined frequency. Levin et al. (20) pointed out that the lose of regular cycle pattern may not be preferable since it brings confusions to travlers. Therefore, the study proposed a model with a fixed phase sequence and maximum cycle length. Other examples of cycle-based MP algorithms include (11, 26).

While the metric plays an important role on the control performance, the ability to measure this metric also influences its use. Mercader et al. (23) argued that queue length can be difficult to obtain in practice and instead proposed a MP algorithm based on vehicular travel time in the previous cycle. The model was validated in a field experiment. Since minimization of travel delay is one of the mostly used objectives in traffic signal control problems, delay-based MP algorithms have also been proposed. Moreover, delay is inherently capacity-aware, i.e., the marginal delay increases with queue length. Wu et al. (27) developed a delay based MP algorithm using the Head-Of-Line (HOL) information, but the proposed model only works for isolated intersections. Dixit et al. (11) proposed a parsimonious delay-based MP and showed that high-quality real-time delay data could be obtained at a cheaper cost than physical sensors required for queue measurement. However, this model cannot relate the queue lengths and delay at an arbitrary time. More recently, Liu and Gayah (15) proposed a delay-based MP (D-MP) that can overcome this drawback. The model divides vehicles on a link into two groups: moving vehicles (at free flow speed) and stopped vehicles. Then, the delay incurred in one time step is equal to the number of stopped vehicles multiplied by the time step size. It is mathematically proved that the model owns the most desirable property of the Original-MP: maximum stability, which means a demand can be accommodated by this algorithm if it can be accommodated by any control policy. Simulation results show that the D-MP performs well under various traffic conditions, including partially connected vehicle environments.

To the best of our knowledge, none of aforementioned models has considered delay equity, measured as the variation of delay experienced among all individual vehicles. This is another common signal control objective that has been widely studied; see (28–30). The lone exception is (27), which is only applicable for isolated intersections. Moreover, while the HOL model generates fairness compared to queue-based MP, it also leads to longer queue lengths. This tradeoff between the fairness and queue lengths can be adjusted by using a weighted sum of the HOL term and queue term as the weight; however, there is not a systematic method to find the optimal coefficients in the weighted sum. In light of this gap in the literature, we propose here a delay-based model that improves both delay equity and average delay under various traffic conditions. The performance of the proposed algorithm, which is referred to as TD-MP, is compared to three benchmark models: Original-MP, D-MP and PWBP. The paper shows the proposed algorithm has the lowest variation in travel delay under all tested scenarios, and it has even lower average delay than D-MP under most scenarios. The performance of all methods is also tested and compared in a Connected Vehicle (CV) environment in which a subset of vehicles are monitored and can contribute to estimates of the MP metrics. The results show the TD-MP is more stable than the baseline models, and it generates both lower traffic delay and higher equity when the penetration rate is below 60%.

The rest of this paper is organized as follows. The next section introduces the general form of a MP algorithm and shows the proposed algorithm along with the baseline algorithms. The subsequent section conducts the simulation and shows the comparison of the control performance between the proposed algorithm and baseline models under various scenarios. We conclude in the last section.

1 **METHODS**

2 This section first introduces the general form of a MP algorithm, focusing on the definitions of weight and
 3 pressure. Then, the baseline models are described, with emphasis on how they differ. Next, we propose the
 4 novel MP algorithm, TD-MP, that can be used to improve delay equity.

5 Useful notations for network configuration in this paper are defined as follows. A link pair (l, m)
 6 that allows vehicle transitions at an intersection is called a movement. The set of link pairs that is served
 7 by phase p at intersection i is denoted by L_i^p . $r(l, m)$ is the turning ratio from link l to link m . $O(l)$ is the
 8 set of allowed movements from link l . ϕ_i is the set of phases at intersection i . $V(l, m)$ is the set of vehicles
 9 of movement (l, m) .

10 **General form of a MP algorithm**

11 In all MP algorithms, the signal timing is determined by the pressure of all phases. In a cycle-less algorithm,
 12 the phase with the maximum pressure is activated for the next step, while in a cycle-based algorithm, the
 13 effective green time is allocated according to the proportion of the pressures. The proposed algorithm is
 14 cycle-less, so we focus on this type in the following. The general form for a pressure of a phase, P_i^p , can be
 15 expressed as:

$$P_i^p = \sum_{(l,m) \in L_i^p} w(l, m) \left(1 - \delta(l, m) \frac{T - e}{T}\right) s(l, m) \quad (1)$$

16 where $w(l, m)$ is the weight of movement (l, m) , T is the pre-defined time step size for signal update, e is
 17 the lost time between phase switch, $\delta(l, m)$ is 0 if movement (l, m) is currently served and 1 otherwise and
 18 $s(l, m)$ is the saturation flow of movement (l, m) . Equation (1) shows that the pressure of a phase is a linear
 19 combination of the product of the weight and saturation flow associated with each movement. The term
 20 $1 - \delta(l, m) \frac{T - e}{T}$ considers the lost time between phase switches. The pressure is dependent on time t ;
 21 however, we omit it from Equation (1) for simplicity. Note the time step for signal update, T , differs from
 22 the time step for traffic state update, which is usually smaller. After obtaining the pressure, the phase with
 23 the largest pressure will be activated for the next time step:

$$P_i^*(t) = \operatorname{argmax}_{p \in \phi_i} P_i^p(t) \quad (2)$$

24 All cycle-less MP variants have the same form for the pressure calculation; they only differ in the
 25 computation of the weight associated with each of the movements. The general form for weight of a
 26 movement can be expressed as

$$w(l, m) = x_1(l, m) - \sum_{(m,n) \in O(m)} r(m, n) x_2(m, n) \quad (3)$$

27 where $x_1(l, m)$ and $x_2(m, n)$ are the upstream and downstream values for selected metric, e.g., number of
 28 vehicles, travel time or traffic delay, etc. The second term in Equation (3) is the weighted average metric
 29 value for the downstream movements using turning ratios. Its main function is to reduce the chance of
 30 activating the phase if the downstream is congested. For example, the Original-MP uses the number of
 31 vehicles as the metric; if $x_2(m, n)$ is high, it means the downstream links are congested so it might not be
 32 optimal to active the corresponding phase. Another function is that a reasonable design of x_1 and x_2 ensures
 33 the maximum stability. A control policy has maximum stability if it can accommodate any demand that can
 34 be accommodated by any other control policy, where accommodation means the number of vehicles in the
 35 network is always upper bounded under the control policy. This property has been proved in certain models,
 36 e.g., the Original-MP (10) and D-MP (15), with infinite queue capacity assumptions. Note that maximum
 37 stability is still an open question if the queue capacity is assumed to be finite. Readers interested in the

1 details of these proofs are referred to (10, 15) for more details. In general, x_1 and x_2 have the same form,
 2 but this is not required. The PWBP and the proposed model both have different expressions for both terms,
 3 which will be explained later.

4

5 **Baseline models**

6 This section shows the expressions of weight of the three baseline models: Original-MP, PWBP and D-MP.
 7 All three models are cycle-less, so we only focus on the weight calculation.

8

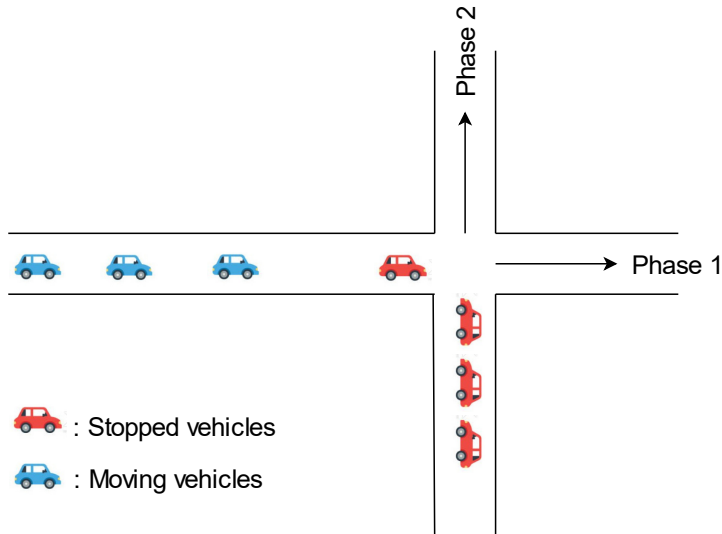
9 *Original-MP*

10 The Original-MP uses point queue models for the traffic states, and the number of vehicles of movements,
 11 $n(l, m)$ is used to calculate weight in Equation (3), which ignores the locations and moving status of
 12 vehicles. It can be expressed as:

$$w(l, m) = n(l, m) - \sum_{(m, n) \in O(m)} r(m, n)n(m, n) \quad (4)$$

13 where $n(l, m)$ is the number of vehicles of movement (l, m) . This model can lead to unreasonable decisions
 14 in some scenarios. For example, Figure 1 shows an intersection of two one-way streets with only straight-
 15 through movements. Although phase 1 has more vehicles on its associated link than phase 2 (four on the
 16 former, three on the latter), it is more reasonable to activate phase 2 rather because the three vehicles on its
 17 link are already queued at the stop line and are waiting to be served. However, the Original-MP will activate
 18 phase 1 since it has a larger number of vehicles, which could waste precious green time at the signal as the
 19 moving vehicles approach the intersection.

20

21
22 **Figure 1. An intersection of two one-way streets**

23

24 *Position-weighted back pressure (PWBP)*

25 To address the issue with vehicle positions in the Original-MP, Li and Jabari (21) proposed a MP model
 26 which involves the location of vehicles on the link in the weight calculation:

$$w_{PWBP}(l, m) = \sum_{i \in V(l, m)} (X(l, m) - x(i, l, m)) - \sum_{(m, n) \in O_m} r(m, n) \sum_{i \in V(m, n)} x(i, m, n) \quad (5)$$

1 where $X(l, m)$ is the link length and $x(i, l, m)$ is the distance of vehicle i from the downstream end of link
 2 l . As Equation (5) shows, the expressions of weights for upstream and downstream movements are different.
 3 For upstream movement, vehicles closer to the downstream node have higher weight because they could
 4 suffer higher control delay if the phase is idle. On the other hand, for downstream movement, vehicles
 5 closer to the upstream node have higher weight because they have more significant impact on the upstream
 6 discharge. Using this method, PWBP activates phase 2 in the example shown in Figure 1, which should
 7 lead to better control performance.

9 Delay-based MP (D-MP)

10 Liu and Gayah (15) proposed a delay-based MP algorithm and demonstrated it outperforms the Original-
 11 MP and other two benchmark models under various scenarios. In the D-MP model, the vehicles on a link
 12 are divided into two groups: moving vehicles and stopped vehicles. Moving vehicles are assumed to always
 13 travel at free flow speed until they join the queue and, thus, all traffic delay is related to the stopped vehicles.
 14 Travel delay incurred in the previous time step was used for the weight calculation in D-MP. Therefore, D-
 15 MP uses an average metric, unlike the Original-MP and PWBP which both use a snapshot metric in the
 16 weight calculation. The weight at the i th time step can be expressed as:

$$w_{D-MP}(l, m, iT) = \sum_{t=(i-1)T+1}^{iT} d(l, m, t) - \sum_{(m, n) \in O_m} r(m, n) \sum_{t=(i-1)T+1}^{iT} d(m, n, t) \quad (6)$$

17 where $d(l, m, t)$ is the delay generated from movement (l, m) in time t .

19 Proposed algorithm

20 Total-delay based MP

21 As demonstrated in (15), the D-MP outperforms three baseline models in average traffic delay, queue length
 22 and network throughput under various scenarios. In this model, the signal phase is selected at a pre-defined
 23 frequency depending on the delay of each movement in the previous time step. However, this means that
 24 the weight for each movement is reset to be zero at the beginning of each step regardless of the cumulative
 25 delay incurred by the current vehicles. Although this method achieves reasonable performance overall, it
 26 may lead to inequitable situations in which one movement experiences extremely large delay to the benefit
 27 of others. This method specifically favors approaches with heavier traffic when demand is unbalanced and
 28 thus approaches with less traffic may experience very high delays. This phenomenon can be explained using
 29 the following example shown in Figure 2. The intersection consists of a one-way street and a two-way
 30 street, and each street only has one lane. Vehicles from the northbound street can either go straight or turn
 31 right; the southbound street allows straight movement and left turns; the eastbound street allows through
 32 movement only. These three movements are served by three individual phases as denoted in Figure 2(a).
 33 Assume vehicles arrive to phase 2 and phase 3 continuously at a fixed rate of 1 veh/s, and that vehicle
 34 arrival rate to phase 1 is 0 veh/s. Also assume the saturation flow for all movements is 2 veh/s, signal phases
 35 are updated every 4 s, and the lost time between phase switches can be ignored. For simplicity, we also
 36 assume all vehicles move at free flow speed when signal is green; i.e., vehicles do not experience delay
 37 during the green time. Let the left side of Figure 2(b) be the initial state at $t = 0$ s; note that one vehicle is
 38 waiting for phase 1, four vehicles are waiting for phase 2, and no vehicles are waiting for phase 3. Consider
 39 the case where the D-MP activates phase 2 for the first time step since it has the largest number of vehicles

in the queue. At time $t = 4$ s, the queue of phase 2 will be cleared since the saturation flow of 2 veh/s is able to just process the initial queue and new arrivals in the first time step. For phase 3, one vehicle arrives in each second. Consequently, there are 4 vehicles waiting for phase 3 at $t = 4$ s. The first vehicle arrives at $t = 1$ so the delay it incurs is 3 s. Similarly, the other three vehicles experience delay of 2 s, 1 s and 0 s, respectively. Therefore, the delay incurred by vehicles of phase 3 in this time step is 6 s. However, for phase 1, the delay is always equal to 4 s in each time step since there is always only a single vehicle waiting in the queue. Therefore, phase 3 is activated at $t = 4$ s. Moving forward, the signal will keep switching between phase 2 and phase 3, and phase 1 will always be idle. Consequently, the vehicle waiting for phase 1 will incur an arbitrarily large delay.

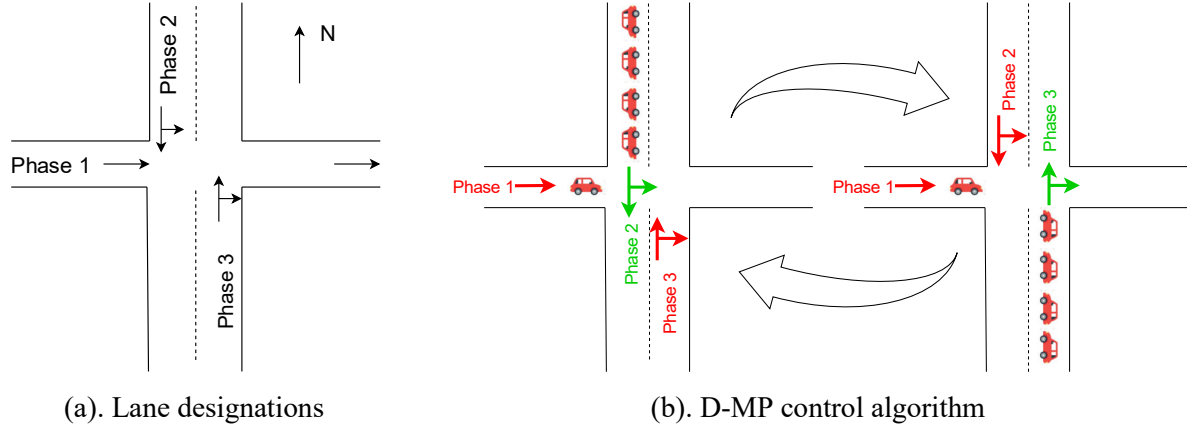


Figure 2 Inequitable control from D-MP

To overcome this drawback, we replace the delay term in Equation (6) with the sum of delay incurred by all vehicles on the link since they join the link. Since we use the total delay from all vehicles, we refer to this model as TD-MP. The weight can be expressed as:

$$w_{TD-MP}(l, m, iT) = \sum_{i \in V(l, m)} d_v(i, l, m) - \sum_{(m, n) \in O_m} \left(r(m, n) \sum_{t=(i-1)T+1}^{iT} d(m, n, t) \right) \quad (7)$$

where $d_v(i, l, m)$ is the delay incurred by vehicle i since it joins movement (l, m) . This should provide improved delay equity by helping to ensure that some vehicles do not experience extremely high delays to benefit others. Considering the example above, the weight for phase 1 is 8s at the beginning of the third time step, which will allow it to be served at $t = 8$ s.

Note we keep the downstream term from D-MP. As mentioned before, the main goal of the downstream term is to avoid activating a phase if the downstream links are all congested. If the downstream link has less vehicles, it should impose less (negative) impact on the weight. However, $d_v(i, l, m)$ considers the cumulative delay since the vehicle joins the link rather than the current level of congestion. As the previous example shows, a downstream link with fewer vehicles can have higher cumulative delay, which makes it unsuitable for the downstream term. Therefore, we use the same downstream term from D-MP which only counts the delay from the previous time step. By using the cumulative delay from all vehicles for the upstream movements, the TD-MP is expected to reduce the traffic delay for approaches with low traffic demand and improve the delay equity. It is worthwhile to mention that Equation (7) does not maintain maximum stability. In general, the maximum stability requires the control policy to serve the busiest phase

1 when making decisions. However, the main purpose of the proposed algorithm is to improve the delay
 2 equity, for which Equation (7) would not always activate the busiest phase, especially when the demand is
 3 unbalanced. As mentioned before, the establishment of maximum stability is under one strong assumption:
 4 the queue capacity of all links is infinite, which is questionable in reality. In addition, the simulation results
 5 in the following sections show that while improving the delay equity, our model can even improve the
 6 overall performance, i.e., reducing delay, compared to all baseline models that have the maximum stability.

7

8 *Modification for work conservative property*

9 A signal control policy is said to be work conservative if the activated phase can serve at least one vehicle
 10 (i.e., at least one served upstream link is not empty and its downstream links are not all full), as long as
 11 there exists at least one vehicle that can be served at the intersection. This property has been discussed in
 12 some MP-based algorithms, e.g., (12, 23). Up to now, the weight definition of the proposed algorithm and
 13 all baseline models cannot ensure the work conservative property. To this end, we change the pressure
 14 expression in Equation (1) to:

$$P_i^p = \sum_{(l,m) \in L_i^p} w(l,m) \left(1 - \delta(l,m) \frac{T - e}{T} \right) s(l,m) - \frac{1}{M \sum_{(l,m) \in L_i^p} (n(l,m) \sum_{(m,n) \in O_m} (Q(m,n) - n(m,n)))} \quad (8)$$

15 where M is a big number and $Q(m,n)$ is the queue capacity of link (m,n) . The MP models with pressure
 16 defined by Equation (8) are work conservative. If an upstream link (l,m) is empty or all its downstream
 17 links are full, the term $n(l,m) \sum_{(m,n) \in O_m} (Q(m,n) - n(m,n))$ is equal to zero. Therefore, if all movements
 18 served by phase p meet this condition, the term $\sum_{(l,m) \in L_i^p} (n(l,m) \sum_{(m,n) \in O_m} (Q(m,n) - n(m,n)))$ is equal
 19 to zero, and we call this an infeasible phase. Consequently, the pressure defined by Equation (8) is negative
 20 infinity, so the infeasible phases cannot be activated by the control policy, as shown by Equation (2) except
 21 all phases are infeasible. The big-M is used to make the second term small, and thus maintain the pressure
 22 for feasible phases. All models become work conservative by using Equation (8) to update signal timing.
 23 Note, in following simulations, if all phases have empty upstream links or fully congested downstream
 24 links, we randomly select a phase to activate at that intersection.

25

26 **SIMULATION TESTS**

27 To validate the proposed algorithm, microscopic traffic simulation tests are conducted using SUMO (31).
 28 Since the proposed TD-MP is an extension of D-MP developed in (15), as a preliminary test, we first
 29 compare these two algorithms for an isolated intersection. Then, we compare the proposed algorithm
 30 against all baseline models on a grid network assuming the full knowledge of the required metrics can be
 31 obtained. Subsequently, the control performance of the proposed algorithm in a partially connected
 32 environment is tested.

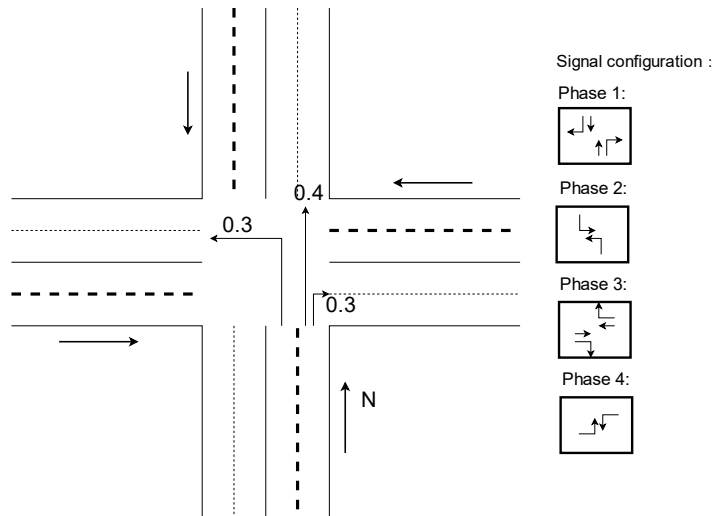
33

34 **Test at an isolated intersection**

35 *Simulation settings*

36 We examine the performance of the proposed model when applied to an isolated intersection, illustrated in
 37 Figure 3. The incoming links are marked by thicker dashed lines, and the arrows showing the travel

1 direction. For each incoming link, the right lane is a shared lane by the right turn and the through movements, 2 and the left lane is for left turn only. Turning ratios are assumed to be identical for all incoming links. The 3 speed limit is set to 20 m/s and the saturation flow is 1800 veh/hr/lane. We use the default car-following 4 model Krauss (32) in SUMO. Available phase options are shown on the right side of the figure. The lost 5 time between phase changes is set to 3s. The signal update time step $T = 5$ s, while the simulation time step 6 is 1s. At the time of each update, TD-MP calculates the pressure as the cumulative delay of all vehicles that 7 are currently on each link since they enter the link. Note that for this isolated intersection, the downstream 8 links are essentially sinks, so we do not include the downstream term in the weight and pressure calculations. 9



10
11 **Figure 3 Single intersection configuration**
12

13 For simplicity, we use equal demands for north-south (NS) and east-west (EW) incoming links, 14 denoted f_{NS} and f_{EW} , respectively. The sum of these two demands is fixed for all simulations and set equal 15 to 1400 veh/hr/lane. To study the delay equity, one balanced and five unbalanced demand scenarios are 16 considered. In all unbalanced scenarios, NS links have higher traffic demand than EW links. Ten runs with 17 different random starting seeds were performed for each scenario. This section serves as a preliminary 18 demonstration for the equity improvement of the proposed algorithm.
19

20 *Results*

21 Figure 4 shows the average delay measured for each individual lane at the intersection. In the legend, L 22 indicates the left-turn-only lane, and RT indicates the shared lane. The x-axis indicates the difference in 23 demand between the NS and EW links. For example, 0 indicates the balanced scenario, in which the demand 24 for all four approaches equals 700 veh/hr, and 200 veh/hr means the demands for NS and EW links are 800 25 veh/hr and 600 veh/hr, respectively. Darker colors are used to represent the results from the D-MP and 26 lighter colors are used for the TD-MP. We consider the distribution of delay across intersection movements 27 as a measure of delay equity. The results reveal that D-MP generates inequitable travel delay even under 28 the balanced scenario, which is caused by the unequal turning ratios. Since there are fewer left turns than 29 right and through movements combined, the delay from the left lanes is significantly higher than the right 30 lanes. Notice that the delay from the NS links decreases as the demand imbalance increases, as it has the 31 heavier load; by contrast, the delay for the EW links increases with the demand imbalance. As a result, the 32 delay variation increases significantly with the level of demand imbalance. The difference in delay for

1 individual movements can be quite large; e.g., when the demand difference is 1000 veh/hr, the delay
 2 difference experienced from the D-MP between vehicles on the EW left-turn lanes and NS through-right
 3 lanes is 59 s, which is 317% of the average delay experience at the intersection.

4 The TD-MP can improve the delay equity effectively, even for the balanced scenario. When the
 5 demand difference is less than or equal to 400 veh/hr, TD-MP produces higher delay for right lanes and
 6 lower delay for left lanes compared to D-MP. Consequently, the delay difference among all lanes is reduced.
 7 When the demand difference exceeds 400 veh/hr, the demand of the left lane from NS direction becomes
 8 higher than the demand of both lanes from EW direction. Accordingly, TD-MP increases the delay of both
 9 lanes from NS direction and reduces the delay of the other direction. Thus, the TD-MP model improves the
 10 delay equity for all tested scenarios.

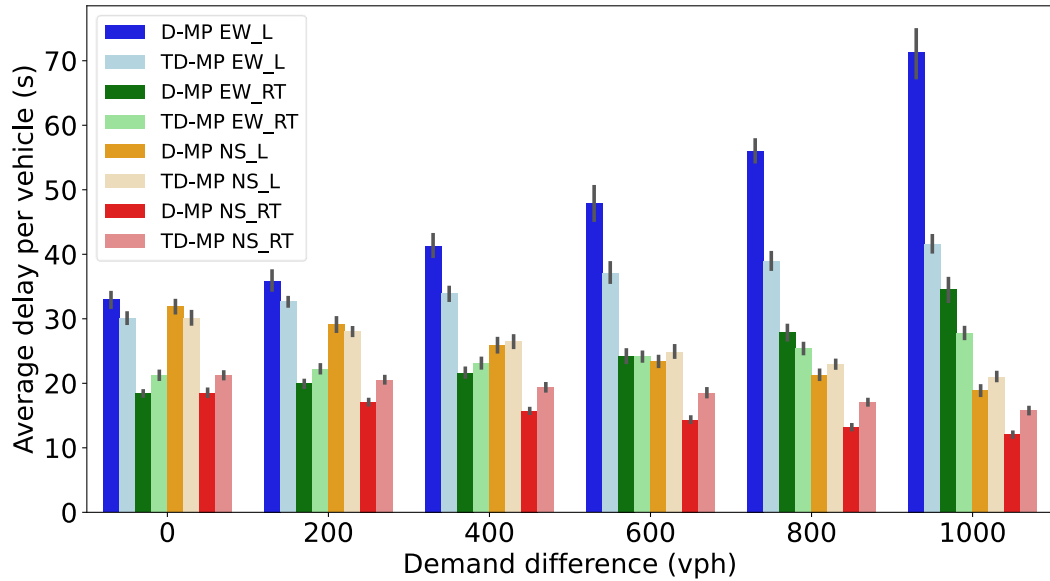


Figure 4 Lane-wise average delay

11
 12 Figure 5 shows the average delay and standard deviation of delay experienced by all vehicles in the
 13 simulation. Figure 5(a) shows that the average delay from TD-MP is larger than that of the D-MP; however,
 14 the amount is small (less than 2 s per vehicle and less than 10% of what is observed in the D-MP) and this
 15 difference diminishes with the level of imbalance. On the contrary, Figure 5(b) shows TD-MP can reduce
 16 the standard deviation in traffic delay considerably; the improvement ranges from 2 s for the balanced case
 17 (13%) to 7 s for the most unbalanced case (35%). Overall, these results demonstrate the power of TD-MP
 18 to improve the delay equity without the significant sacrifice of overall mobility for a single intersection.
 19 The next section will demonstrate that these benefits can be further improved when the TD-MP is applied
 20 network-wide.
 21
 22

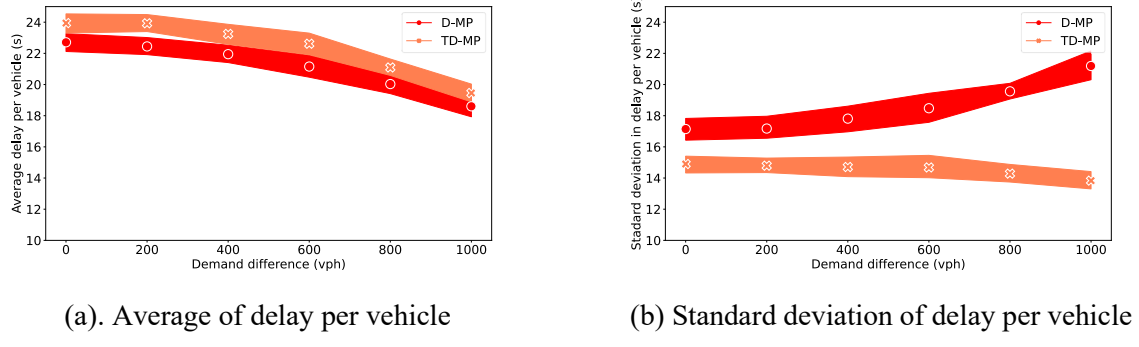


Figure 5 Comparison of delay per vehicle

Test on a grid network

Simulation settings

To further demonstrate the benefits of the TD-MP model, its performance is tested on an idealized 4×4 grid network, illustrated in Figure 6. The phase pattern, turning ratio and lane configuration are the same as the single intersection. Similarly, all NS links have the same demand, and all EW links have the same demand. We tested three demand levels for $f_{NS} + f_{EW}$: 1200 veh/hr, 1400 veh/hr and 1500 veh/hr. We refer to these three levels as the low, medium, and high demand levels. For each demand level, one balanced scenario and five unbalanced scenarios are considered.

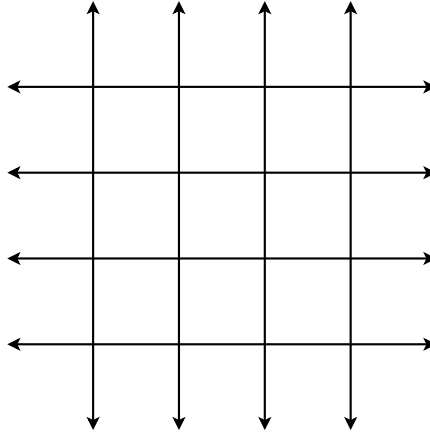


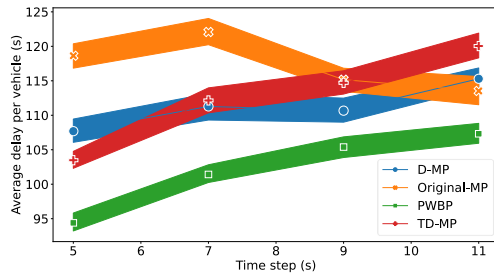
Figure 6 A grid network

Simulation-based optimal time step

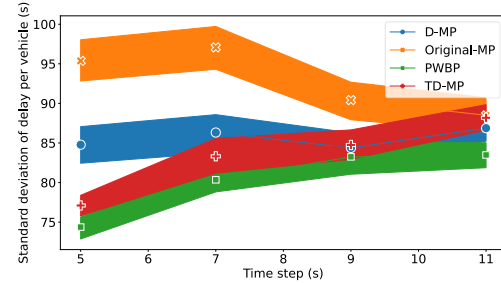
Liu and Gayah (15) showed that the update time step is critical for MP-based control. Thus, the optimal update time steps are needed for each method for a fair comparison of their performance. To this end, all models were applied using four values for time step (5 s, 7 s, 9 s and 11 s) for two scenarios under the high demand level: a balanced scenario in which $f_{NS} = f_{EW} = 750$ veh/hr; and, an unbalanced scenario in which $f_{NS} = 1050$ veh/h and $f_{EW} = 450$ veh/h. The average and standard deviation of delay per vehicle for each model/time step combination are shown in Figure 7. 10 simulations with different random starting seeds were performed, and the shaded area of the curves correspond to the confidence interval for the mean

values. The results reveal that, for the unbalanced scenario, all models have an optimal time step of 5 s at which both the average delay and standard deviation are the lowest. For the balanced scenario, 5 s is also optimal for TD-MP, D-MP and PWBP. The Original-MP has different optimal values; the difference in performance across time steps is much smaller than that in the unbalanced scenario. The possible reason that the Original-MP has a larger optimal time step when the demand is balance is that when the time step is very small, e.g., 5 s, the controller could switch phases too frequently because the number of vehicles is sensitive to traffic state, which can generate high time losses and lead to poor performance. Specifically, when the demand is balance, we can reasonably assume the numbers of vehicles from all approaches are similar. Therefore, a phase activated in previous time step tends to have less vehicles than other phases at the next one or two time steps. As a result, the signal phase changes very frequently which will create unnecessary phase switches and high time losses that lead to poor performance. This issue is diminished by other three models because the metrics are more insensitive to the number of vehicles. In addition, the most scenarios we will test are unbalanced. Therefore, to ensure the fairness, we use 5 s for all models.

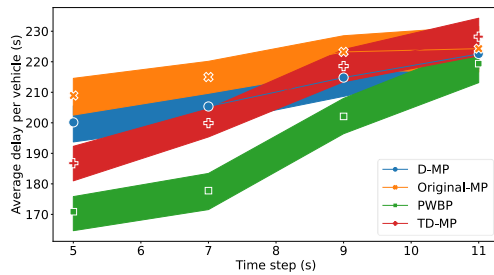
14



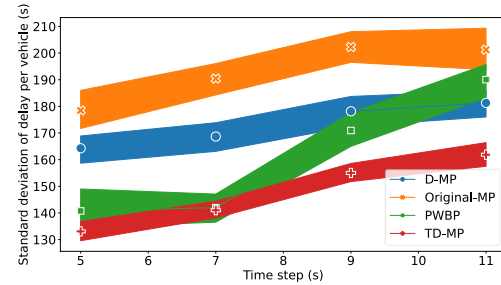
(a). Average for balanced case



(b). Standard deviation for balanced case



(c). Average for unbalanced case



(d). Standard deviation for unbalanced case

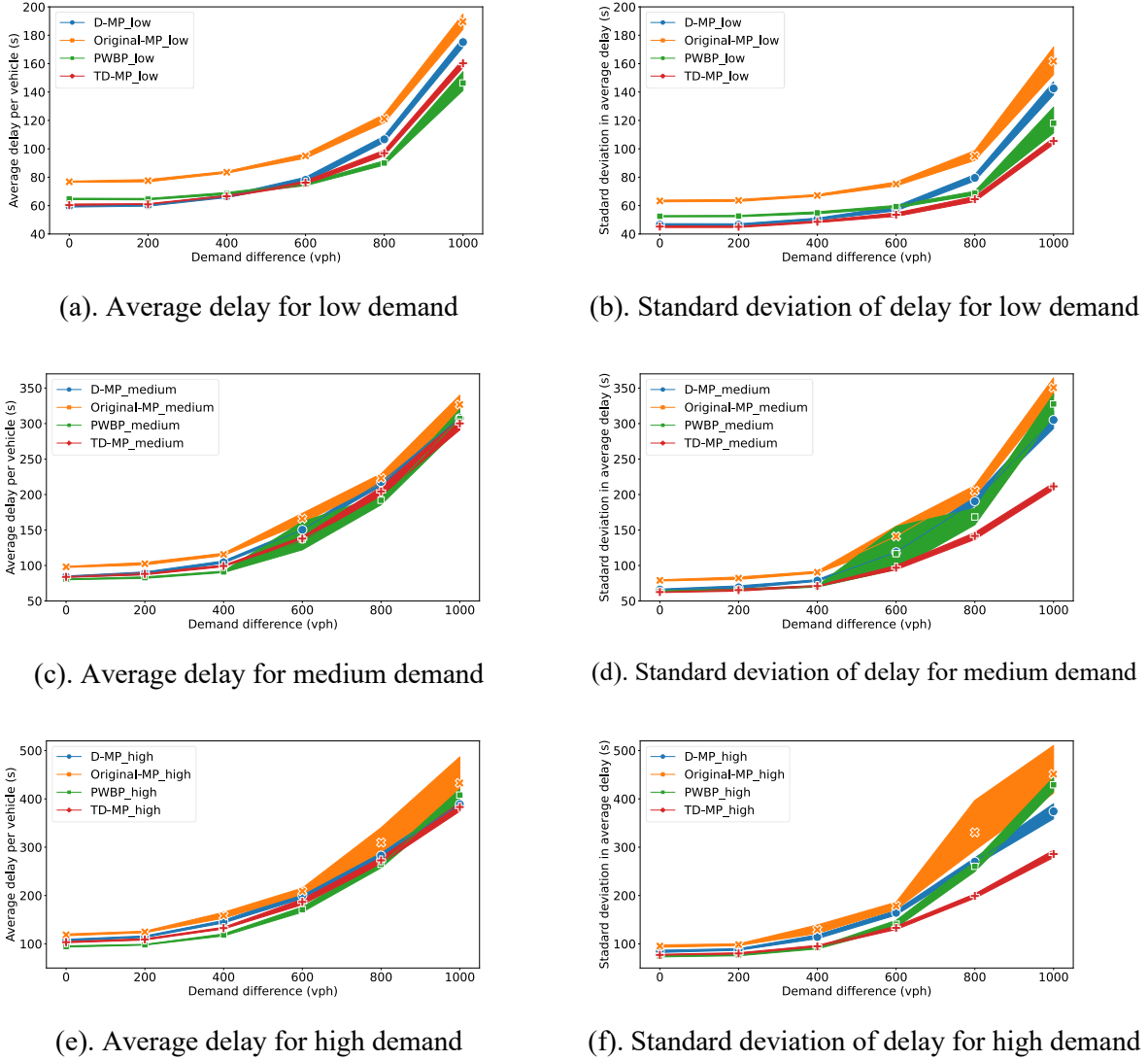
15

16

17 Results with full knowledge of required metrics under stable demand

18 Figure 8 shows the average delay and standard deviation of delay obtained from all models for the three
 19 demand levels. For each scenario, although the time headway of vehicle generations is random, the average
 20 arrival rate is fixed through the whole simulation. Therefore, we refer to this demand pattern as stable
 21 demand. For all demand levels and models, the average and variation of delay increase with the level of
 22 imbalance. The Original-MP has the highest values for both metrics in all scenarios. This is not unexpected
 23 since it uses a snapshot metric to determine the signal timing, and it treats all vehicles on a link as the same
 24 while locations and moving status are crucial for the performance. With the increase in travel demand, the
 25 average queue length increases, and the non-queued vehicles will decrease. Thus, the negative influence

1 from this treatment is diminished. Therefore, the relative increases in the average delay as demand increases
 2 between the Original-MP and other models is reduced, especially for the balanced scenarios.



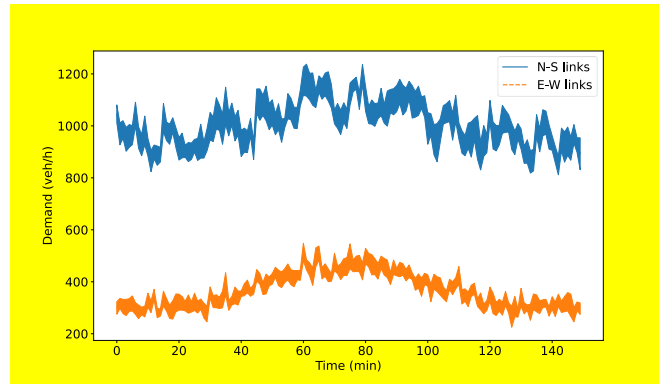
3 **Figure 8 Performance comparison under stable demand**

4

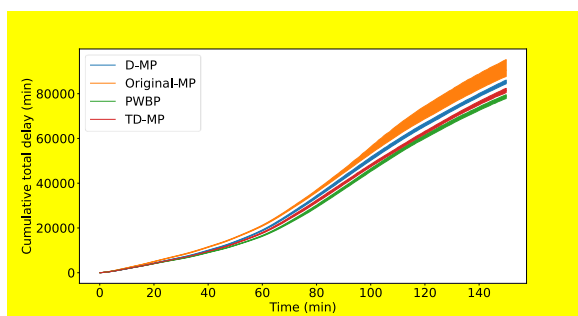
5 Interestingly, the proposed TD-MP has the lowest delay for several cases tested; specifically, for
 6 demand differences less than 600 veh/h under low demand levels or demand differences higher than 800
 7 veh/h under the medium and high demand levels. For other scenarios, the PWBP has the lowest average
 8 delay, but the average delay difference among the D-MP, TD-MP and PWBP models are negligible.
 9 However, the standard deviation from TD-MP is considerably smaller than all three baseline models for
 10 most cases, which suggests that the TD-MP provides better delay equity than all other methods. The
 11 differences are starker for the highly unbalanced scenarios and under higher demand levels. Figure 8 leads
 12 to a similar conclusion as the single intersection case study: for a network, TD-MP can improve the delay
 13 equity significantly, and this improvement does not come at the any significant cost of the overall mobility.

1 **Results with full knowledge of required metrics under unstable demand**

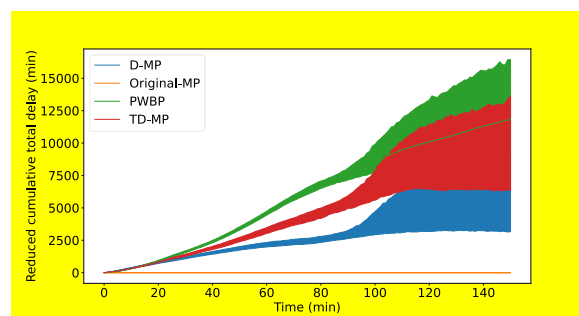
2 The previous section demonstrated the control performance of the TD-MP under stable demand. However,
 3 since adaptive signal control strategies are designed to tackle real-time traffic conditions, it is critical to
 4 investigate the control performance under unstable demand. To this end, we create a typical scenario in
 5 which the average demand increases from a low starting level to a high level and then drops back to the
 6 low level. We assume the demand difference between NS entry links and EW entry links is 600 veh/h for
 7 the whole simulation. In addition to this variation in the average demand, we assume under unstable
 8 demand, the real arrival rate changes every 5 minutes and follows a normal distribution with a mean equal
 9 to the average demand in that interval and a standard deviation equal to 5% of the mean. For example,
 10 if $f_{NS} = 900$ for the first 20 minutes, a sample is drawn every 5 minutes from the distribution $N(900, 45)$ to
 11 be used as the arrival rate for the corresponding 5-minute interval. Figure 9 shows the unstable demand
 12 pattern generated using this method.

13 **Figure 9 Unstable demand**

14 Figure 10(a) shows the cumulative delay for all models under unstable demands, and for the
 15 visualization purpose, Figure 10(b) shows the delay reduction from the other three models compared to the
 16 Original-MP. As expected, since the MP algorithms use the pre-defined metric value which solely depends
 17 on the current traffic states on the local links to determine the signal timing, the uncertainties do not have a
 18 significant impact on the control performance. Similar to the scenarios under stable demand (when the
 19 demand difference is 600 veh/h), the PWBP has the lowest delay while the Original-MP has the worst
 20 performance; furthermore, TD-MP reduces delay compared to D-MP.
 21



22 (a). Cumulative delay

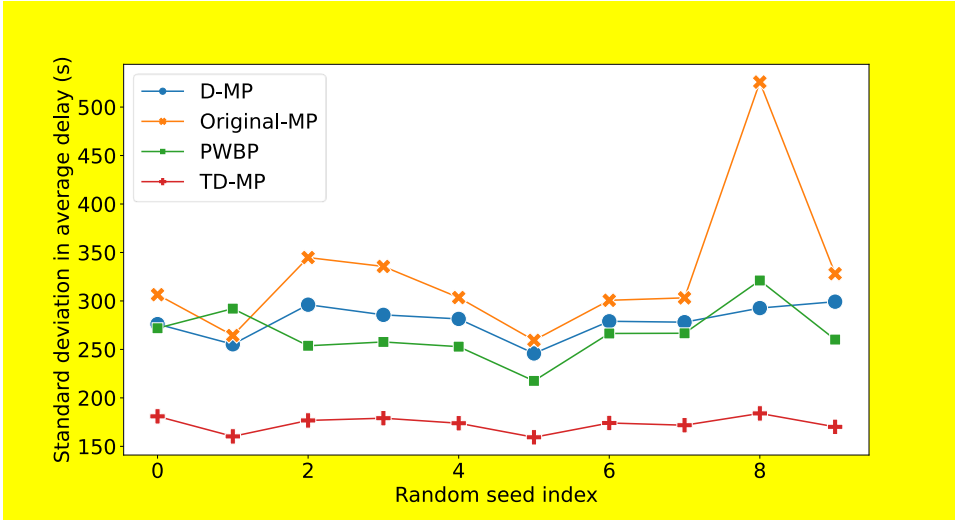


23 (b). Reduced delay compared to the Original-MP

24 **Figure 10 Delay comparison under unstable demand**

25 Figure 11 shows the standard deviation of travel delay per vehicle in all 10 simulation runs. It shows
 26 that for all random seeds, TD-MP can improve the delay equity significantly compared to all baseline
 27 models. PWBP has a better delay equity than D-MP and the Original-MP for most random seeds while it

1 generates higher delay variation for a few random seeds. Above all, this section shows that the MP-based
 2 algorithms are robust to the randomness in the travel demand.



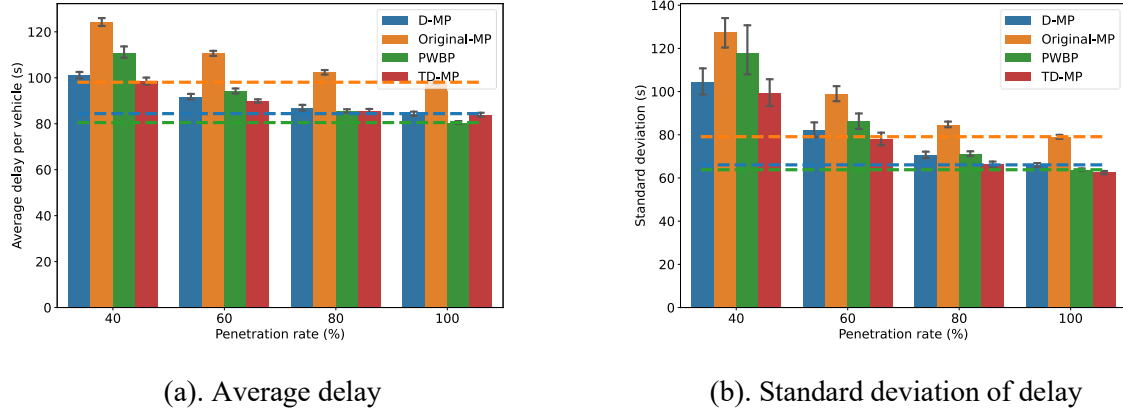
3
 4 **Figure 11 Delay variation under unstable demand**

5 *Results in a partially connected vehicle environment*

6 The results shown in the previous section are obtained when perfect information is available to compute
 7 metrics required to implement all MP models. However, this requires perfect sensing across the network,
 8 which is not realistic or expected. Compared to the baseline models, it is more challenging to obtain the
 9 pressure for TD-MP since it requires the exact arrival time and departure time of each vehicle on a link for
 10 the total delay computation. Thanks to the advancement and increasing deployment of connected vehicles
 11 (CVs), traffic states can also be obtained through the communication with the CVs without the help of other
 12 equipment. However, since a fully connected environment is not expected to occur in the near future, it is
 13 critical to test the model performance in a partially connected vehicle environment. In this case, traffic
 14 states may be estimated based on the information provided by only a portion of vehicles that serve as CVs,
 15 and the information from other vehicles is ignored. For example, if there are 2 connected vehicles and 5
 16 non-connected vehicles on a link, the value for the metric of the Original-MP, which is the number of
 17 vehicles, is 2.

18 To this end, we considered five CV penetration rates $\lambda \in \{20, 40, 60, 80, 100\}$ used to provide
 19 inputs for the required metrics in all MP algorithms. For simplicity, we only investigated the balanced
 20 scenario and one unbalanced scenario (with demand difference of 600 vph) for the medium demand level.
 21 (To have a relatively fair comparison, we do not use the most unbalanced scenario in which the TD-MP
 22 outperforms other models considerably in terms of delay equity.) The influence of the penetration rate is
 23 shown in Figure 9 and Figure 10. The horizontal dashed lines indicate the values of the baseline models in
 24 a fully connected environment, i.e., $\lambda = 100$. The error bars indicate the standard error across the 10
 25 random seeds. Both the average delay and the standard deviation when $\lambda = 20$ are significantly larger than
 26 other values. For example, the average delay of PWBP and TD-MP, which are the best models in a fully
 27 connected environment, from the balanced scenario is equal to 883 s and 186 s, respectively. This suggests
 28 that an extremely low penetration is not sufficient to obtain these metrics. Therefore, to have a better
 29 visualization, the results of $\lambda = 20$ are omitted.

1



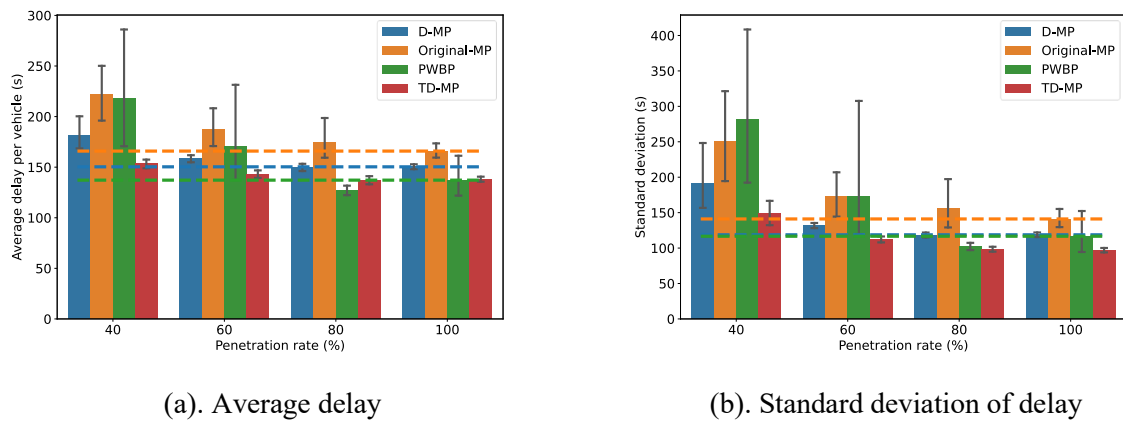
(a). Average delay

(b). Standard deviation of delay

Figure 12 Comparison in a CV environment with balanced demand

2

3



(a). Average delay

(b). Standard deviation of delay

Figure 13 Comparison in a CV environment with unbalanced demand

4

5

6

7

8

9

10

11

12

In line with our expectation, both the average delay and delay variation of all models worsen with a decrease in the penetration rate. This influence of penetration rate is more significant for the unbalanced scenario than the balanced scenario, i.e., for a given reduction in the penetration rate, the increase in the two metrics for the unbalanced scenario is higher than the balanced scenario. In addition, for both demand scenarios, this impact of the penetration rate is more significant when the penetration rate is low. For instance, for the unbalanced scenario shown in Figure 10 (b), the increase in the standard deviation when the penetration rate changes from 60% to 40% is much more significant than the increase when the penetration rate changes from 100% to 80%.

13

14

15

16

17

18

19

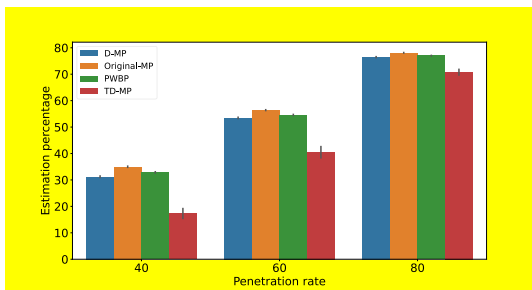
20

For the comparison of model performance, the proposed TD-MP provides the best delay equity for all penetration rates under both unbalanced and balanced scenarios. It also generates the lowest average delay when penetration rate is equal to or lower than 60%. This is reasonable as the TD-MP is able to better account for “lone” vehicles at an approach (see example associated with Figure 2), which is more likely under smaller penetration rates. When the penetration rate is higher, the average delay from the TD-MP is still very close to the minimum value, which is achieved by the PWBP. Note although PWBP has the lowest average delay when the penetration rate is higher than 80%, its performance worsens drastically when the penetration rate decreases. When the penetration rate drops to 40%, it even generates larger delay variation

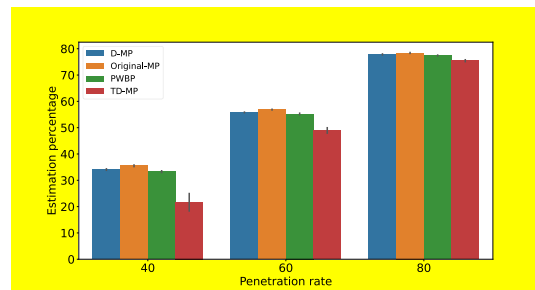
than the Original-MP, which has the worst control performance under all other scenarios. PWBP requires both the number of vehicles and the positions of all vehicles for the weight calculation. In a highly connected vehicle, the second information is beneficial for the control performance since it provides more detailed and accurate traffic state information. However, when the penetration rate is low, the high randomness can result in large errors in the weight estimates and worsen the control performance.

In addition to the comparison of the average delay and the standard deviation, TD-MP is also more stable responding to both the traffic randomness, which is reflected by the error bars in Figure 9 and Figure 10, and the penetration rate, which is reflected by the changes in both metrics for a change in the penetration rate, than other models. This is a very desirable property for a signal control algorithm.

To investigate the estimation error from the connected vehicle in the pressure calculation, we compute the ratio of the sum of the value estimated from the connected vehicle over all links and all steps during the whole simulation to the corresponding value computed from all vehicles. Figure 14 shows the ratio (in percentage) of the estimation under both demand scenarios tested above. The original-MP has the highest estimation ratio while the TD-MP has the lowest. This is not unexpected. The reason is that TD-MP and D-MP use average metrics, i.e., delay in each time step and total delay incurred by current vehicles, while the Original-MP and PWBP use snapshot metrics, i.e., number of vehicles and position weighted number of vehicles at the instants of signal update. Assume there are one non-connected vehicle and one connected vehicle on a link at the first time step, and the connected vehicle leaves in the second time step. For the Original-MP, the ratio in these two time steps is equal to $\frac{1+0}{2+1} = 0.33$; however, the ratio for the TD-MP is equal to $\frac{1+0}{2+2} = 0.25$. Therefore, TD-MP has a lower estimation ratio than the Original-MP due to this faster increase in the denominator in the estimation ratio calculation. It can be explained in the same manner for other models as well. Although the TD-MP has the lowest estimation ratio, it has the best performance in both average delay and delay equity under various conditions. The reason is twofold: First, total-delay is a better metric in nature to reflect the traffic condition than other metrics in various traffic conditions; second, it is the relative estimation accuracy among all phases instead of the estimation accuracy itself that determines the control performance. Although the estimation ratio of TD-MP is lower, the connected vehicles are randomly distributed in the system, so it is reasonable to assume the estimation ratio for all approaches is very similar in the long-run. Therefore, TD-MP is still able to select the phase with the actual maximum pressure in certain time steps. Consequently, compared to other algorithms, the TD-MP can provide the correct control for enough time steps to outperform the baseline algorithms.



(a). Balanced demand



(b). Unbalanced demand

Figure 14 Estimation ratio from connected vehicles

Overall, in a CV environment, the performance of all the tested MP-based models improves with an increase in the number of CVs. It shows the proposed TD-MP has the best performance in both the average delay and delay equity for most scenarios. Moreover, the TD-MP is a more stable control policy responding to the randomness in both traffic conditions and penetrate rate.

1 **CONCLUSIONS**

2 This paper develops a new MP model using the sum of delay over all vehicles since they join a link as the
3 metric to compute the weight. The proposed model is compared to multiple other MP-based signal control
4 methods, including the Original-MP, PWBP and recently proposed D-MP model. The simulation results
5 suggest that the proposed model can improve equity significantly, especially for highly unbalanced traffic
6 conditions, while simultaneously keeping the average delay almost as low as other models. Simulations
7 also reveal that when data on travel times, delays and vehicle positions are only available from a subset of
8 vehicles – as would be the case in a Connected Vehicle environment, the proposed model is more stable
9 than the Original-MP and PWBP and demonstrates similar stability to the D-MP model. Further, the
10 proposed TD-MP provides the highest delay equity for all tested penetration rate and the lowest average
11 delay when the penetration rate is equal to or lower than 60%.

12 The existing MP algorithms control traffic operation through signal timings. Thanks to the
13 development and increasing popularity of Autonomous Vehicles (AVs), this emerging technology has the
14 potential to boost the efficiency further. Therefore, proposing a method to combine the MP algorithm and
15 the control of AVs is a promising future research direction. In addition to travel time, traffic delay and
16 queue, other measure of effectiveness such as number of stops and fuel consumption is another point that
17 needs to be investigated. This paper focuses on the time-step based MP algorithm in which the controller
18 switches phase at a fixed frequency. Other cycle-based MP algorithms (20, 23, 33) have also been proposed,
19 in which the phase sequence and duration are adjusted every cycle. Since the minimum green time is usually
20 imposed, they are expected to have less intensive delay inequity. However, the green allocation in such
21 models is proportional to the pressure, which can lead to delay inequity as well. Therefore, it is another
22 interesting topic to investigate the delay equity in cycle-based MP algorithms.

23
24 **ACKNOWLEDGMENTS**

25 This research was supported by NSF Grant CMMI-1749200.

26

27 **AUTHOR CONTRIBUTIONS**

28 The authors confirm contribution to the paper as follows: study conception and design: H. Liu, V. Gayah;
29 analysis and interpretation of results: H. Liu, V. Gayah; draft manuscript preparation: H. Liu, V. Gayah.
30 All authors reviewed the results and approved the final version of the manuscript.

REFERENCES

1. Olszewski, P. Overall Delay, Stopped Delay, and Stops at Signalized Intersections. *Journal of transportation engineering*, Vol. 119, No. 6, 1993, pp. 835–852.
2. Mirchandani, P., and L. Head. A Real-Time Traffic Signal Control System: Architecture, Algorithms, and Analysis. *Transportation Research Part C: Emerging Technologies*, Vol. 9, No. 6, 2001, pp. 415–432. [https://doi.org/10.1016/S0968-090X\(00\)00047-4](https://doi.org/10.1016/S0968-090X(00)00047-4).
3. Abdulhai, B., R. Pringle, and G. J. Karakoulas. Reinforcement Learning for True Adaptive Traffic Signal Control. *Journal of Transportation Engineering*, Vol. 129, No. 3, 2003, pp. 278–285. [https://doi.org/10.1061/\(ASCE\)0733-947X\(2003\)129:3\(278\)](https://doi.org/10.1061/(ASCE)0733-947X(2003)129:3(278)).
4. Cai, C., C. K. Wong, and B. G. Heydecker. Adaptive Traffic Signal Control Using Approximate Dynamic Programming. *Transportation Research Part C: Emerging Technologies*, Vol. 17, No. 5, 2009, pp. 456–474. <https://doi.org/10.1016/j.trc.2009.04.005>.
5. Wei, H., G. Zheng, V. Gayah, and Z. Li. A Survey on Traffic Signal Control Methods. *arXiv preprint arXiv:1904.08117*, 2019.
6. Gartner, N. H. OPAC: A Demand-Responsive Strategy for Traffic Signal Control. *Transportation Research Record*, No. 906, 1983, pp. 75–81.
7. Robertson, D. I., and R. D. Bretherton. Optimizing Networks of Traffic Signals in Real Time—the SCOOT Method. *IEEE Transactions on vehicular technology*, Vol. 40, No. 1, 1991, pp. 11–15.
8. Chow, A. H. F., R. Sha, and S. Li. Centralised and Decentralised Signal Timing Optimisation Approaches for Network Traffic Control. *Transportation Research Part C: Emerging Technologies*, Vol. 113, No. November 2018, 2020, pp. 108–123. <https://doi.org/10.1016/j.trc.2019.05.007>.
9. Tassiulas, L., and A. Ephremides. Stability Properties of Constrained Queueing Systems and Scheduling Policies for Maximum Throughput in Multihop Radio Networks. 1990.
10. Varaiya, P. Max Pressure Control of a Network of Signalized Intersections. *Transportation Research Part C: Emerging Technologies*, Vol. 36, 2013, pp. 177–195. <https://doi.org/10.1016/j.trc.2013.08.014>.
11. Dixit, V., D. J. Nair, S. Chand, and M. W. Levin. A Simple Crowdsourced Delay-Based Traffic Signal Control. *PLoS ONE*, Vol. 15, No. 4, 2020, pp. 1–12. <https://doi.org/10.1371/journal.pone.0230598>.
12. Gregoire, J., X. Qian, E. Frazzoli, A. De La Fortelle, and T. Wongpiromsarn. Capacity-Aware Backpressure Traffic Signal Control. *IEEE Transactions on Control of Network Systems*, Vol. 2, No. 2, 2015, pp. 164–173. <https://doi.org/10.1109/TCNS.2014.2378871>.
13. Wu, J., D. Ghosal, M. Zhang, and C. N. Chuah. Delay-Based Traffic Signal Control for Throughput Optimality and Fairness at an Isolated Intersection. *IEEE Transactions on Vehicular Technology*, Vol. 67, No. 2, 2018, pp. 896–909. <https://doi.org/10.1109/TVT.2017.2760820>.
14. Xiao, N., E. Frazzoli, Y. Li, Y. Wang, and D. Wang. Pressure Releasing Policy in Traffic Signal Control with Finite Queue Capacities. *Proceedings of the IEEE Conference on Decision and Control*, Vol. 2015-Febru, No. February, 2014, pp. 6492–6497. <https://doi.org/10.1109/CDC.2014.7040407>.
15. Liu, H., and V. V. Gayah. A Novel Max Pressure Algorithm Based on Traffic Delay. *Transportation Research Part C: Emerging Technologies*, Vol. 143, 2022. <https://doi.org/10.1016/j.trc.2022.103803>.
16. Xu, T., S. Barman, M. W. Levin, R. Chen, and T. Li. Integrating Public Transit Signal Priority into

Max-Pressure Signal Control: Methodology and Simulation Study on a Downtown Network. *Transportation Research Part C: Emerging Technologies*, Vol. 138, No. March, 2022. <https://doi.org/10.1016/j.trc.2022.103614>.

17. Wang, X., Y. Yin, Y. Feng, and H. X. Liu. Learning the Max Pressure Control for Urban Traffic Networks Considering the Phase Switching Loss. *Transportation Research Part C: Emerging Technologies*, Vol. 140, No. May, 2022, p. 103670. <https://doi.org/10.1016/j.trc.2022.103670>.
18. Kouvelas, A., J. Lioris, S. A. Fayazi, and P. Varaiya. Maximum Pressure Controller for Stabilizing Queues in Signalized Arterial Networks. *Transportation Research Record: Journal of the Transportation Research Board*, Vol. 2421, No. 1, 2014, pp. 133–141. <https://doi.org/10.3141/2421-15>.
19. Le, T., P. Kovács, N. Walton, H. L. Vu, L. L. H. Andrew, and S. S. P. Hoogendoorn. Decentralized Signal Control for Urban Road Networks. *Transportation Research Part C: Emerging Technologies*, Vol. 58, 2015, pp. 431–450. <https://doi.org/10.1016/j.trc.2014.11.009>.
20. Levin, M. W., J. Hu, and M. Odell. Max-Pressure Signal Control with Cyclical Phase Structure. *Transportation Research Part C: Emerging Technologies*, Vol. 120, No. October, 2020, p. 102828. <https://doi.org/10.1016/j.trc.2020.102828>.
21. Li, L., and S. E. Jabari. Position Weighted Backpressure Intersection Control for Urban Networks. *Transportation Research Part B: Methodological*, Vol. 128, 2019, pp. 435–461. <https://doi.org/10.1016/j.trb.2019.08.005>.
22. Lioris, J., A. Kurzhanskiy, and P. Varaiya. Adaptive Max Pressure Control of Network of Signalized Intersections. *IFAC-PapersOnLine*, Vol. 49, No. 22, 2016, pp. 19–24. <https://doi.org/10.1016/j.ifacol.2016.10.366>.
23. Mercader, P., W. Uwayid, and J. Haddad. Max-Pressure Traffic Controller Based on Travel Times: An Experimental Analysis. *Transportation Research Part C: Emerging Technologies*, Vol. 110, No. December 2019, 2020, pp. 275–290. <https://doi.org/10.1016/j.trc.2019.10.002>.
24. Varaiya, P. The Max-Pressure Controller for Arbitrary Networks of Signalized Intersections. In *Advances in Dynamic Network Modeling in Complex Transportation Systems*, Springer, pp. 27–66.
25. Wei, H., C. Chen, G. Zheng, K. Wu, V. Gayah, K. Xu, and Z. Li. Presslight: Learning Max Pressure Control to Coordinate Traffic Signals in Arterial Network. 2019.
26. Mercader, P., W. Uwayid, and J. Haddad. Max-Pressure Traffic Controller Based on Travel Times: An Experimental Analysis. *Transportation Research Part C: Emerging Technologies*, Vol. 110, 2020, pp. 275–290.
27. Wu, J., D. Ghosal, M. Zhang, and C.-N. Chuah. Delay-Based Traffic Signal Control for Throughput Optimality and Fairness at an Isolated Intersection. *IEEE Transactions on Vehicular Technology*, Vol. 67, No. 2, 2017, pp. 896–909.
28. Liang, X. (Joyce), S. I. Guler, and V. V. Gayah. An Equitable Traffic Signal Control Scheme at Isolated Signalized Intersections Using Connected Vehicle Technology. *Transportation Research Part C: Emerging Technologies*, Vol. 110, 2020, pp. 81–97. <https://doi.org/10.1016/J.TRC.2019.11.005>.
29. Hitchcock, O., and V. V. Gayah. Methods to Reduce Dimensionality and Identify Candidate Solutions in Multi-Objective Signal Timing Problems. *Transportation Research Part C: Emerging Technologies*, Vol. 96, 2018, pp. 398–414.
30. Lertworawanich, P., M. Kuwahara, and M. Miska. A New Multiobjective Signal Optimization for Oversaturated Networks. *IEEE Transactions on Intelligent Transportation Systems*, Vol. 12, No. 4,

2011, pp. 967–976.

31. Lopez, P. A., M. Behrisch, L. Bieker-Walz, J. Erdmann, Y.-P. Flötteröd, R. Hilbrich, L. Lücken, J. Rummel, P. Wagner, and E. Wießner. Microscopic Traffic Simulation Using SUMO. 2018.
32. Krauß, S. Microscopic Modeling of Traffic Flow: Investigation of Collision Free Vehicle Dynamics. 1998.
33. Dixit, V., D. J. Nair, S. Chand, and M. W. Levin. A Simple Crowdsourced Delay-Based Traffic Signal Control. *PLoS one*, Vol. 15, No. 4, 2020, p. e0230598.